JETIR.ORG ISSN: 2349-5162 | ESTD Year : 2014 | Monthly Issue
JOURNAL OF EMERGING TECHNOLOGIES AND INNOVATIVE RESEARCH (JETIR)
An International Scholarly Open Access, Peer-reviewed, Refereed Journal

Triton X-100 micellar effects and Kinetic models in the oxidation of Phenylsulfinylacetic acids by Iron(III) polypyridyl complexes

[1*]R. Jeevi Esther Rathnakumari, [2]C. Kavitha, [3]J. Janet Sylvia Jaba Rose [4]P. Subramaniam, [5]V.Vetriselvi.
[1*]Head & Associate Professor, [2]Head & Assistant Professor
[1]Department of Chemistry, Nazareth Margoschis College, Nazareth-628617, Tamil Nadu, India
[2]Department of Chemistry, Aditanar College of Arts and Science, Tiruchendur-628216, Tamil Nadu, India

ABSTRACT

Oxidative decarboxylation of phenylsulfinylacetic acids (PSAAs) by iron(III) polypyridyl complexes in nonionic surfactant Triton X-100 (TX-100) medium has been investigated spectrophotometrically. From the observed Michaelis–Menten kinetics and fractional order dependence on PSAA an initial intermediate formation between PSAA and $[Fe(NN)_3]^{3+}$ is confirmed. Non-linear concave upward Hammett plots were obtained on applying the Hammett substituent constants to the overall rate constants obtained in TX-100 medium. A suitable mechanism has been proposed involving the formation of Diphenyl sulphone as the product. The observed increase in rate with increase in concentration of TX-100 at low concentrations clearly shows that the reaction takes place in micellar medium and both the reactants are associated or incorporated into micellar phase.The various kinetic models like Menger Portnoy, Piszkiewicz, Raghvan and Srinivasan and Berezin were applied to study the quantitative aspects of reactivity in TX-100 medium.

Keywords: Iron(III) polypyridyl complexes, Electron transfer reactions, Menger-Portnoy model, Piszkiewicz model, Raghvan and Srinivasan model, Berezin model;
*Corresponding author. Tel.: +91 9486251734, E-mail address: jeeviesther@gmail.com (R. Jeevi Esther Rathnakumari)

1. INTRODUCTION

Reactions conducted in aqueous micellar media have created much attention of researchers because of unique reactivity in the media which is not attained in an organic solvent. Surfactants are amphipathic molecules having hydrophobic and hydrophilic properties. When these surfactant molecules are dissolved in water they can achieve segregation of their hydrophobic portions from the solvent by self-aggregation. The aggregation products, known as micelles, are responsible for altering the rates of organic reactions in aqueous-surfactant solutions. Aqueous micellar solutions can alter the kinetics **(**Gangwar & Rafiquee, 2007), yield (Shrikhande et al 2008) as well as the selectivity (Nagaonkar & Bhagwat, 2007) of many organic reactions to a higher extent compared to the reactions carried out in organic solvents. The substrates attain a suitable orientation in a micelle due to the dual nature of micelles. The hydrophobic core of micelles solubilizes sparingly soluble substrates, intermediates and products in water (Pawar & Bhagwat, 2012).

Non-ionic detergents have neutral and hydrophilic head groups. They are considered as mild surfactants due to their ability to break protein-lipid, lipid-lipid associations but not protein-protein interactions. Therefore, proteins are solubilized and isolated in their native and active form, retaining their protein interactors. Triton X-100 is a typical non-ionic surfactant and it is a perfect choice for most immune precipitation experiments. TX-100 has a hydrophilic polyethylene oxide chain and an aromatic hydrocarbon hydrophobic head group. The hydrocarbon group is a 4-(1,1,3,3-tetramethylbutyl) phenyl group .

Recently Pal and co-workers (2002) have indicated that the surface of the protein is similar to a micellar surface and the study of such reactions in a micellar medium throws more light on the details of electron transfer reaction in the biological systems. In the present study, the kinetics of the electron transfer reactions between PSAA and $[Fe(NN)_3]^{3+}$were studied in the absence and presence of nonionic surfactant (TX-100) and the various kinetic models are proposed to explain the Triton X-100 micellar effects .

2. EXPERIMENTAL

2.1 Synthesis of Fe(III) polypyridyl $[Fe(NN)_3]^{3+}$ complexes and preparation of Phenylsulfinylacetic acids

Fe(III) polypyridyl complexes $[Fe(NN)_3]^{3+}$ were prepared by the oxidation of corresponding Fe(II) tris(pyridyl) complexes with lead dioxide in sulphuric acid medium (Adaikalasamy et al 2003). The preparation of $[Fe(NN)_3]^{3+}$ must be done in highly acidic medium in order to get better yield. Finally Fe(III) complexes were precipitated as per-chlorate salts. The purity of the complexes was checked from their IR and absorption spectra. The tris(pyridyl) complexes of Fe(II) were obtained by known

procedure (Balakumar et al 1995). The structure and the abbreviation of iron(III) polypyridyl complexes used in the present study are shown in Figure 1. Stock Solutions of Fe(III) complexes were made up in concentrated perchloric acid and were diluted with aqueous acetonitrile just before initiating the kinetic run. In order to avoid the decomposition of complexes, stock solutions were kept in refrigerator. PSAA, meta- and para-substituted PSAAs were prepared from the corresponding phenylthioacetic acid (PTAA) by the controlled oxidation with hydrogen peroxide (Deepalakshmi et al 2014). PSAAs were purified by recrystallization from ethyl acetate–benzene mixture and their purities were checked by melting point and LC-MS. The recrystallized samples were stored in vacuum desiccator in order to avoid the decomposition with moist air. The structure of substituted phenylsulfinyl acetic acids used in this work is shown in Figure 2.

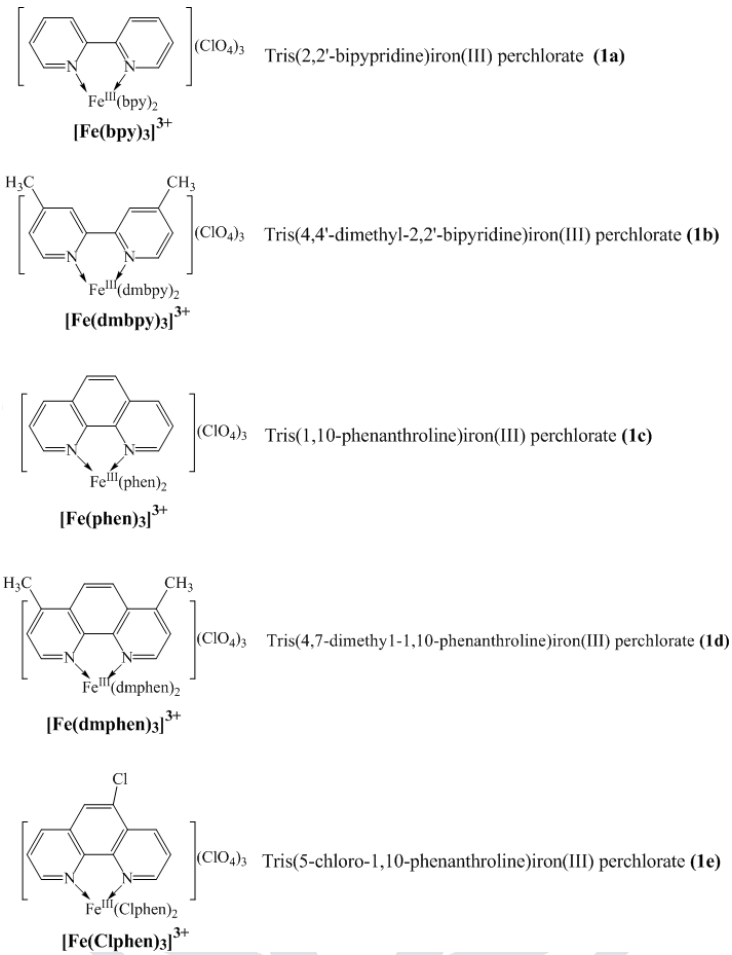

Figure 1. Structure of iron(III) polypyridyl complexes.

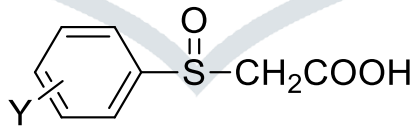

Where Y = *p*-F, *p*-Cl, *p*-Br, *m*-F, *m*-Cl, *m*-Br, H, *m*-Me, *p*-Et, *p*-Me, *p*-*t*.Bu, *p*-OEt, *p*-OMe

Figure 2. Structure of substituted phenylsulfinyl aceticacids.

2.2 Kinetics in the presence of TX-100

The kinetic studies of the reactions between PSAAs and $[Fe(NN)_3]^{3+}$ were carried out in the presence of non-ionic micelle, TX-100 above its CMC value i.e., in the range of 0.001 M to 0.15 M. The reported CMC of TX-100 is 3×10^{-4} M (Frescura et al 1995). The reactions were followed spectrophotometrically by measuring the increase in absorbance of the product, $[Fe(NN)_3]^{2+}$ formed during the reaction. All kinetic measurements were performed under pseudo-first-order conditions with PSAA atleast 10 folds in excess over the $[Fe(NN)_3]^{3+}$ in the presence of TX-100 at 303 K. Due to solubility problem, the reactions in TX-100 were carried out in 97% H_2O- 3% CH_3CN (v/v) medium. Similar solvent systems in many sulfoxidation reactions studies under micellar conditions have been reported (Subramaniam & Thamil Selvi, 2014 and 2015). Perchloric acid was used to maintain $[H^+]$ and sodium perchlorate was used to maintain the ionic strength. The pseudo-first-order rate constants were calculated from the slope of the linear plots of log $(A_\infty - A_t)$ *vs.* time.

2.3 Product analysis

The reaction mixtures containing PSAA and $[Fe(bpy)_3]^{3+}$ / $[Fe(phen)_3]^{3+}$ in 1:1 molar ratio under the experimental conditions were kept aside for two days. After the completion of the reaction, the organic solvent was removed under reduced pressure, extracted with chloroform and dried over anhydrous sodium sulfate. The product obtained after the removal of chloroform was identified as diphenyl disulfone which was characterized by FT-IR and GC-MS spectral studies.

3. RESULTS AND DISCUSSION

3.1 Rate dependence on [PSAA] in TX-100 medium

The pseudo-first-order rate constants computed at different concentrations of PSAA are presented in Table 1 for complexes **1a** and **1c**. The analysis of rate data shows that the pseudo-first order rate constants increase steadily with [PSAA].

Table 1. Effect of [PSAA], [**1a]** and [**1c**] on the rate of TX-100 mediated reactions.

10^3 [PSAA] (M)	10^4 $[Fe(NN)_3]^{3+}$ (M)	10^4 k_1 (s^{-1})	10^2 k_{ov} ($M^{-1})^n$ (s^{-1})
		1a	
3.0	4.0	5.65 ± 0.02	7.83 ± 0.03
5.0	4.0	9.12 ± 0.06	8.20 ± 0.05
10.0	4.0	15.8 ± 0.04	7.91 ± 0.02
20.0	4.0	27.5 ± 0.08	7.63 ± 0.02
30.0	4.0	41.7 ± 0.10	8.18 ± 0.02
10.0	2.0	24.5 ± 0.02	12.2 ± 0.01
10.0	8.0	9.71 ± 0.04	4.84 ± 0.02
		1c	
3.0	4.0	6.10 ± 0.12	1.74 ± 0.03
5.0	4.0	8.65 ± 0.04	1.84 ± 0.01
10.0	4.0	12.6 ± 0.02	1.80 ± 0.01
20.0	4.0	18.5 ± 0.04	1.76 ± 0.01
30.0	4.0	23.5 ± 0.08	1.78 ± 0.01
10.0	2.0	16.8 ± 0.06	2.39 ± 0.01
10.0	8.0	8.12 ± 0.04	1.16 ± 0.01

$[H^+]$ = 0.5 M; μ = 0.6 M; [TX-100] = 5×10^{-2} M; solvent = 97% H_2O-3% CH_3CN (v/v).

The pseudo-first order plots at different initial [PSAA] with **1a** and **1c** are presented in Figure 3 . Further linear plots are obtained when log k_1 is plotted against log [PSAA] for complexes **1a** and **1c** (Figure 4). The slope values are found to be fractional values. The k_2 values calculated using $k_2 = k_1/[PSAA]$ were not constant. Therefore, the overall rate constants were calculated using the relation $k_{ov} = k_1/[PSAA]^{order}$ which are found to be constant. All these facts prove that the order of PSAA for the reactions in TX-100 is fractional.

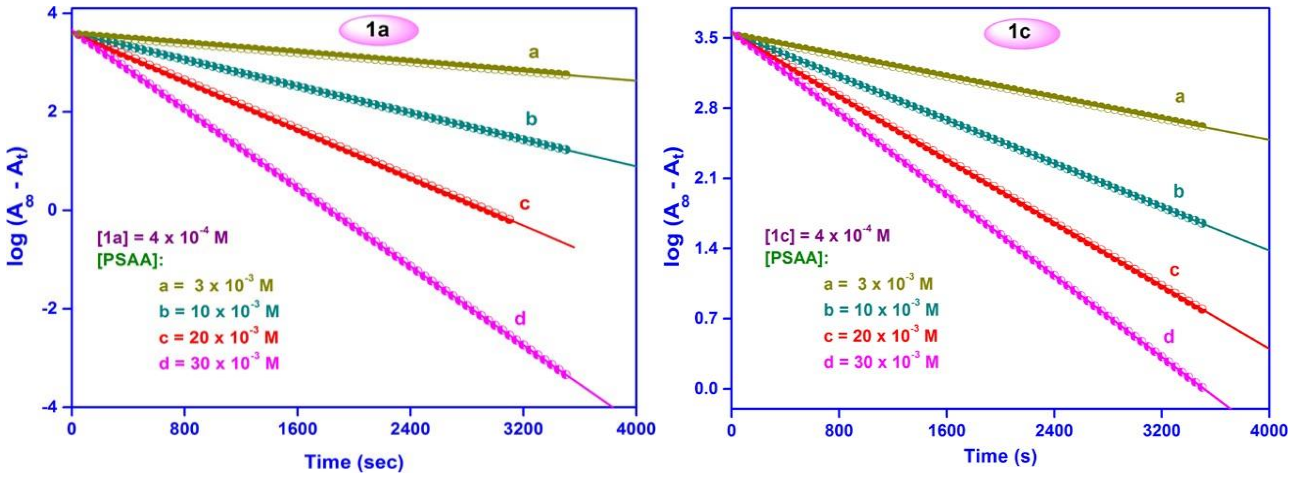

Figure 3. Progress of the reaction at different [PSAA] in TX-100 medium.

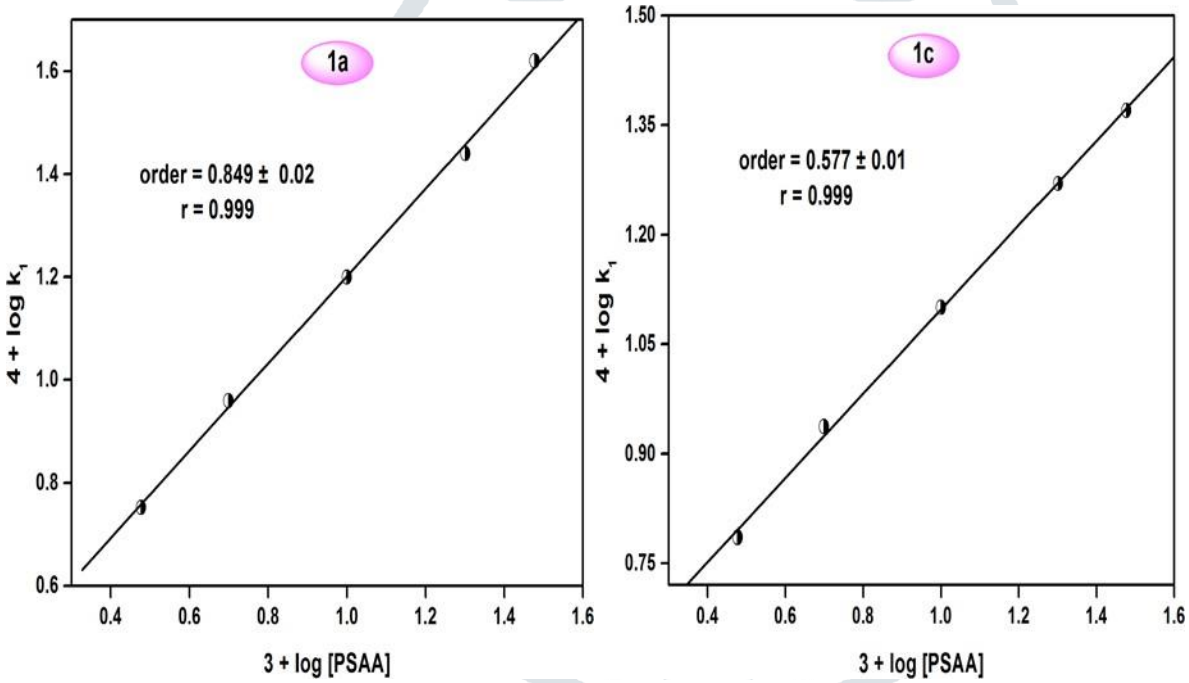

Figure 4. Order plot for PSAA with **1a** and **1c** in TX-100 medium.

The linear plots with finite intercept on the rate axis obtained in the double reciprocal plots of k_1 *vs.* [PSAA] (Figure 5), confirm the Michaelis-Menten kinetics i.e., formation of an intermediate between reactant molecules before the rate determining step.

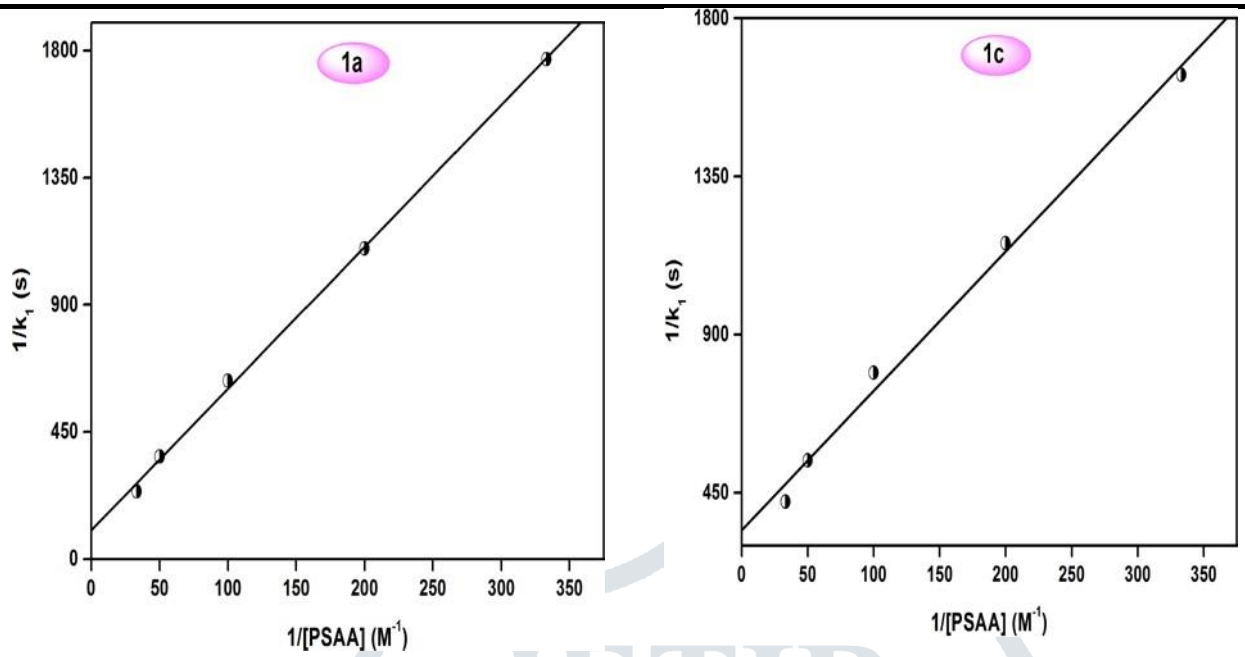

Figure 5. Michaelis-Menten plot for PSAA with **1a** and **1c** in TX-100 medium.

By applying Michaelis-Menten equation,

$$1/k_1 = 1/k + K_m/k\,[PSAA]$$

The values of k and K_m were evaluated from the slope and intercept of the double inverse plot of k_1 against [PSAA]. The evaluated K_m values are found to be 5.32×10^{-2} M and 1.33×10^{-2} M for **1a** and **1c** respectively. The calculated low values of Michaelis-Menten constant ensures strong binding of PSAA to the iron(III) polypyridyl complexes during intermediate formation in TX-100 medium.

3.2 Rate dependence on $[Fe(NN)_3]^{3+}$ in TX-100

The progress of the reaction i.e., log $(A_\infty - A_t)$ against time at different $[Fe(NN)_3]^{3+}$ is shown in Figure 6. The pseudo-first-order rate constants calculated from the above plots at different initial concentrations of $[Fe(NN)_3]^{3+}$ are tabulated (Table 1). From the data, it is concluded that the rate constants decrease with increase in $[Fe(NN)_3]^{3+}$ concentration. The same trend is also observed for the reaction in aqueous and in SDS medium. As in other cases, the reason for the deceleration in rate may be due to the formation of inactive hydrated complex (Schmid & Han, 1983) or oxo-bridged diiron complex (Hey 1982) followed by the decrease in the concentration of reactive species. The explanation and the formation of the above inactive species have been reported in a earlier paper (Subramaniam et al 2016). Among the iron (III) polypyridyl complexes, $[Fe(phen)_3]^{3+}$ is less reactive than $[Fe(bpy)_3]^{3+}$.

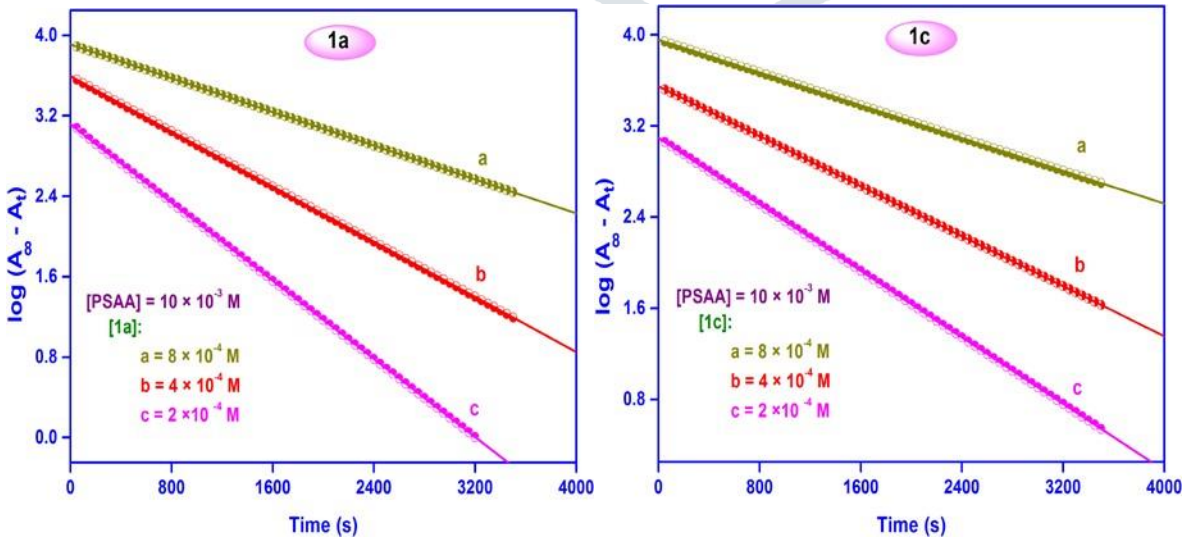

Figure 6. Progress of the reactions at different [**1a**] and [**1c**] with PSAA in TX-100.

3.3 Rate dependence on $[H^+]$

The effect of variation of hydrogen ion concentration on the TX-100 mediated electron transfer reaction between PSAA with **1a** and **1c** were carried out by varying the concentration of perchloric acid. The electron transfer rate increases feebly with an increase in $[H^+]$. The mild rate acceleration can be explained by the stabilization of sulfoxide radical cation at high $[H^+]$.

3.4 Dependence of TX-100 on rate

A series of kinetic runs were carried out with varied concentrations of TX-100 from 3×10^{-3} M to 15×10^{-2} M at constant $[Fe(NN)_3]^{3+}$, $[H]^+$, μ, [PSAA] and temperature. Though the reaction rate is found to be linearly accelerated with increase in concentration of TX-100 at low concentration region, the rate constant reaches a maximum and then decreases at higher concentration of TX-100 for the complexes **1a** to **1d**. However, in the case of **1e** the rate constant increases without any maxima and rate retardation. The observed results are presented in Table 2 and Figure 7. The results also reveal that the accelerating effect ofTX-100 is only marginal in complexes **1a** to **1d**, while in complex **1e**, TX-100 shows a tremendous catalytic effect.

Table 2. Effect of [TX-100] on the rate of reaction between PSAA and the complexes ***1a-1e.***

10^2 [TX-100] (M)	$10^4 k_1$ (s^{-1})				
	1a	**1b**	**1c**	**1d**	**1e**
0	7.14 ± 0.04	3.63 ± 0.08	8.33 ± 0.02	1.69 ± 0.01	13.3 ± 0.06
0.8	7.54 ± 0.08	3.79 ± 0.02	8.34 ± 0.08	1.77 ± 0.01	13.9 ± 0.08
0.9	7.66 ± 0.11	3.89 ± 0.12	8.45 ± 0.04	1.89 ± 0.02	14.7 ± 0.12
1.0	8.25 ± 0.02	4.15 ± 0.04	8.56 ± 0.06	2.13 ± 0.01	16.8 ± 0.08
2.0	8.46 ± 0.01	4.26 ± 0.06	9.40 ± 0.02	2.20 ± 0.04	17.5 ± 0.14
3.0	8.66 ± 0.14	4.31 ± 0.08	10.3 ± 0.05	2.29 ± 0.01	18.6 ± 0.06
4.0	11.4 ± 0.21	5.64 ± 0.14	11.2 ± 0.07	3.23 ± 0.04	47.9 ± 0.18
5.0	15.8 ± 0.03	5.97 ± 0.04	12.6 ± 0.02	3.73 ± 0.02	90.5 ± 0.22
7.0	14.6 ± 0.05	6.44 ± 0.02	13.5 ± 0.01	3.99 ± 0.03	138 ± 0.24
9.0	14.2 ± 0.02	6.15 ± 0.06	14.9 ± 0.06	3.88 ± 0.01	176 ± 0.18
10	13.5 ± 0.06	5.64 ± 0.01	17.5 ± 0.03	3.15 ± 0.04	196 ± 0.26
12	12.2 ± 0.07	5.04 ± 0.04	16.3 ± 0.01	2.74 ± 0.01	215 ± 0.16
15	11.6 ± 0.05	4.42 ± 0.06	15.1 ± 0.03	2.08 ± 0.05	244 ± 0.28

[PSAA] = 1×10^{-2} M; [**1a-1e**] = 4×10^{-4} M; $[H^+]$ = 0.5 M; μ = 0.6 M; [TX-100] = 5×10^{-2} M; solvent = 97 % H_2O - 3 % CH_3CN (v/v).

Similar rate acceleration with increase in TX-100 concentration was observed in the oxidation of diphenyl sulphide (Balakumar et al 2012) with iron (III) polypyridyl complexes in TX-100 medium.

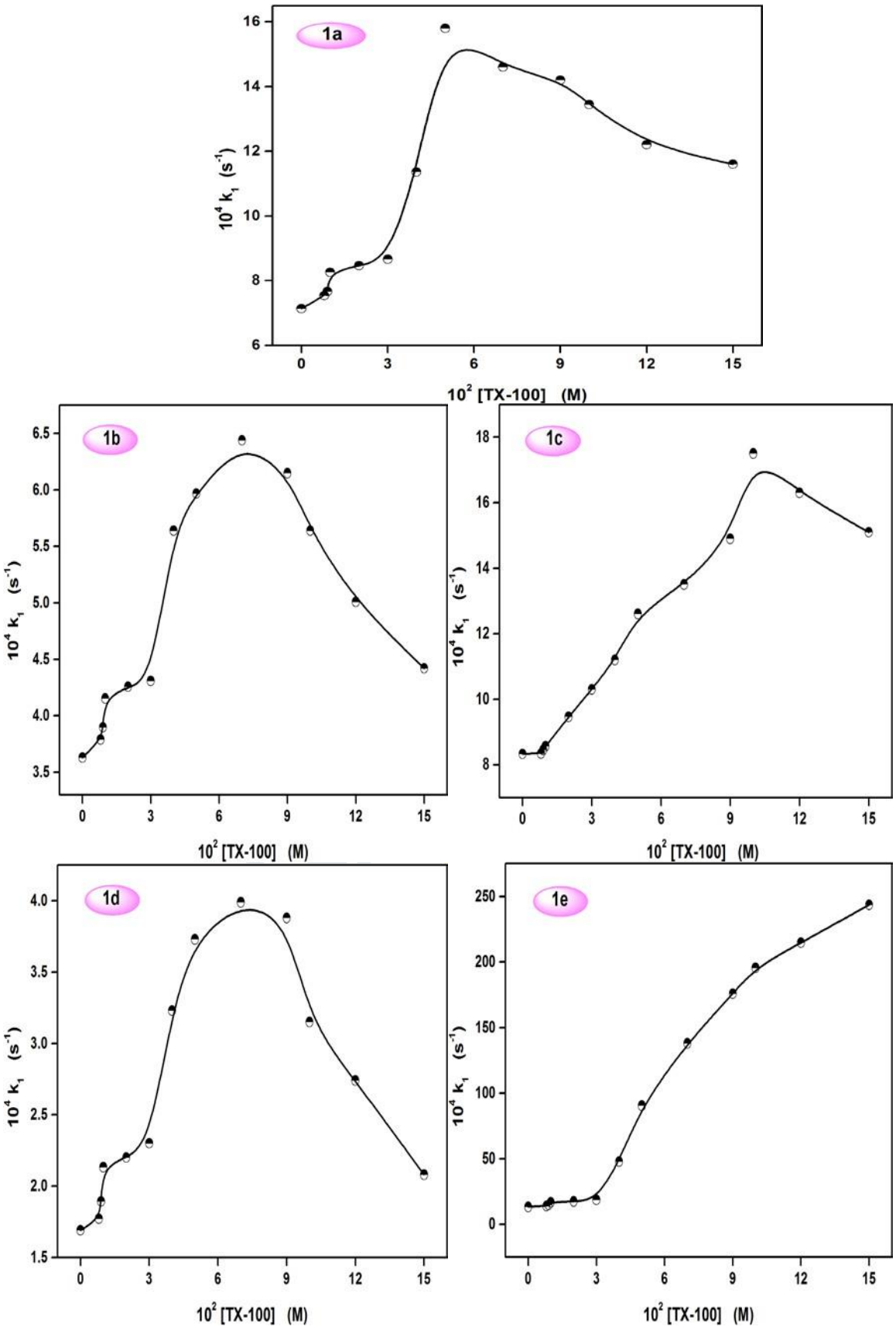

Figure 7. Variation of rate constants with [TX-100].

The rates of dioxygenase reaction of mononuclear iron(III) complexes were significantly higher in TX-100 (Anitha & Palaniandavar 2011) due to the binding of cation of the iron (III) complex with the neutral head group of TX-100. Rate enhancement was also observed with TX-100 for the chromic acid oxidation of dimethyl sulfoxide to dimethyl sulfone (Rumki et al 2015) and oxidative degradation of D-sucrose by N-bromosuccinimide (Singh 2012). Rate acceleration of the reaction at low concentrations and reaching a plateau at higher concentrations of TX-100 was observed in the oxidation of methionine (Altaf & Jaganyi 2013) by colloidal MnO_2.

The retardation of rate in the oxidation of *p*-anisaldehyde by chromic acid in TX-100 medium (Saha et al 2013) was explained by the low concentration of protons needed for the reaction in the miceller phase and a small concentration of intermediate neutral ester formed in the aqueous phase. The ester enters in to the miceller phase by hydrophobic interaction.

3.5 Rate dependence of substituted PSAAs in TX-100 medium and Thermodynamic parameters

The analysis of the substituent effect can give more information about the nature of the transition state intermediates and the mechanism of the electron transfer. Hence the rate of the reaction is examined with several *meta*- and *para*-substituted PSAAs with **1a** and **1c** at three different temperatures *viz*., 293 K, 303 K and 313 K. Non-linear concave upward Hammett plots were obtained on applying the Hammett substituent constants to the overall rate constants obtained in TX-100 medium. The ERG fall on one side of the curve with large negative ρ value and the EWGfall on the other side with low positive ρ value. This indicates that the substituents have accelerating effect on the rate of the reaction. The ρ^+ and ρ^- values obtained from Hammett plots (Figure 8) along with the overall rate constants for the complex **1a is** tabulated in Table 3 .

Table 3. Overall rate constants and thermodynamic parameters for the oxidation of *para*- and *meta*-substituted PSAAs by **1a** in TX-100 medium.

X	$10^2k_{ov}(M^{-1})^n(s^{-1})$			$\Delta^{\ddagger}H$	$-\Delta^{\ddagger}S$
	293K	303K	313K	$kJmol^{-1}$	$JK^{-1}mol^{-1}$
p-F	5.49 ± 0.08	10.5 ± 0.03	18.0 ± 0.12	42.8 ± 0.54	46.4 ± 1.89
p-Cl	12.9 ± 0.12	17.9 ± 0.11	25.5 ± 0.06	23.2 ± 0.45	106 ± 1.59
p-Br	14.3 ± 0.16	19.3 ± 0.10	26.8 ± 0.22	21.4 ± 0.58	111± 2.04
m-F	23.1 ± 1.02	28.1 ± 0.15	35.6 ± 0.46	14.3 ± 1.89	132 ±6.64
m-Cl	26.4 ± 1.04	31.4 ± 0.47	38.9 ± 1.88	11.9 ± 2.50	139 ± 8.79
m-Br	29.2 ± 0.56	34.2 ± 2.05	41.7 ± 0.61	10.6 ± 2.35	142± 8.26
H	4.84 ± 0.08	7.91 ± 0.06	17.3 ± 0.22	46.2 ± 0.82	35.7± 2.90
m-Me	7.92 ± 0.44	12.9 ± 0.66	20.4 ± 0.74	33.6 ± 3.32	74.6± 11.7
p-Et	44.7 ± 0.32	49.6 ± 0.82	57.2 ± 0.64	6.74 ± 0.84	152± 2.97
p-Me	82.4 ± 1.36	87.4 ± 2.88	94.9± 1.02	2.69± 1.61	160± 568
ρ^+	2.19 ± 0.07	1.56 ± 0.05	1.11±0.05		
R	0.998	0.998	0.995		
ρ^-	-7.64 ± 0.49	-6.48±0.52	-5.54 ± 0.55		
R	0.990	0.984	0.975		

[PSAA]=1×10^{-2}M; [**1a**]=4×10^{-4}M; [H^+] = 0.5M; μ=0.6M; [TX-100]=5×10^{-2}M;
Solvent = 97% H_2O = 3% CH_3CN(v/v).

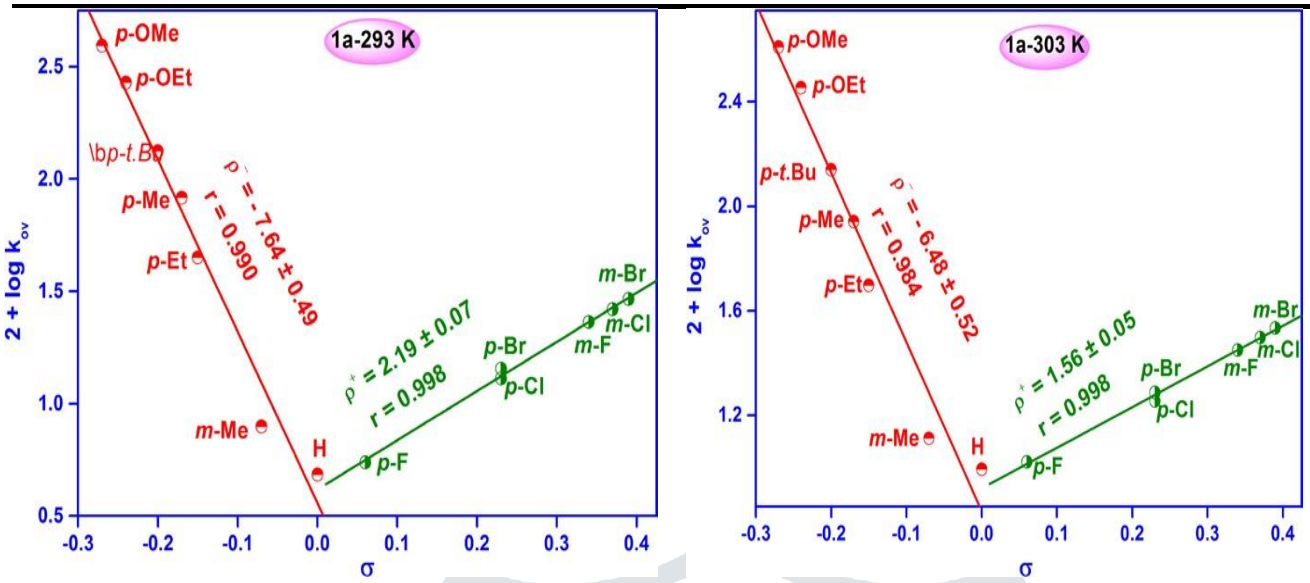

Figure 8. Non-linear Hammett plot in TX-100 medium for **1a** at different temperatures.

The observed trend of pronounced rate acceleration by ERG than EWG indicates the involvement of more positively polarised sulfoxide center of PSAA in the transition state than in the reactant. Similar high ρ^- values are obtained for the reactions in aqueous and SDS mediated reactions of PSAAs with complexes **1a** and **1c** [Jeevi Esther Rathnakumari et al 2024 and Subramaniam et al 2016). Such high ρ^- values are also observed in many sulfoxidation studies (Alhaji, et al 2011).

The overall rate constants for the substituted PSAAs fit Eyring's equation excellently and the thermodynamic parameters are calculated from the Eyring's plot. The reaction is characterized by low enthalpy of activation and appreciable negative entropy ofactivation implying that the activated complex has a specific orientation and the values observed in the present study are of the magnitude, expected for a bimolecular nucleophilic attack of organic sulfur compounds (Thenraja et al 2002). The validity of isokinetic relationship is tested with the observed $\Delta^{\ddagger}H$ and$\Delta^{\ddagger}S$ values as per the Eq.1.

$$\Delta^{\ddagger}H = \Delta^{\ddagger}H + \beta\Delta^{\ddagger}S \qquad (1)$$

Where β is the isokinetic temperature at which all the substituents in a given series have the same reactivity. The isokinetic temperature computed is found to 386 K for **1a** and 366 K for **1c** which is higher than the experimental temperature.

3.6 Mechanism

The kinetic results along with spectral results show that the reaction mechanism (Scheme-1) in the presence of TX-100 remains the same as that in aqueous medium (Subramaniam et al 2016). The rate enhancement observed in the electron transfer reaction between PSAA and $[Fe(NN)_3]^{3+}$ in TX-100 may be due to the hydrogen bonding and hydrophobic interaction which occurs between the surfactant and reactants.

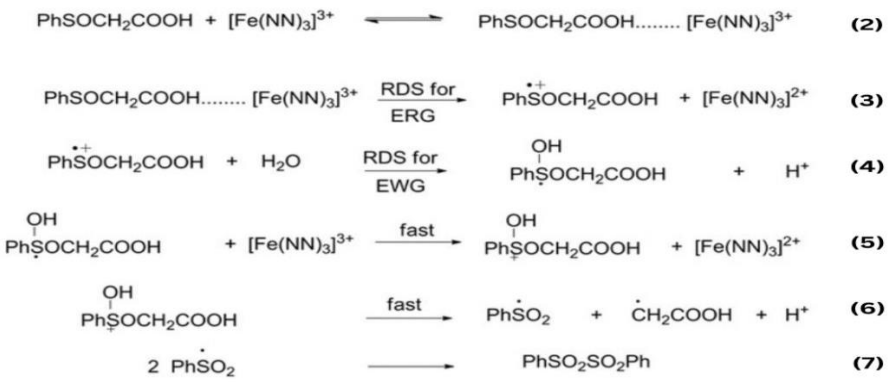

Scheme 1. Mechanism of the reaction in TX-100 medium.

As a result of nucleophilic attack of PSAA on $[Fe(NN)_3]^{3+}$, a positive charge is developed on the sulfur atom of PSAA in the intermediate. On the basis of the above discussion and the observed rate acceleration by both electron withdrawing and electron donating substituents, two different rate determining steps have been proposed on the basis of stabilization of the positive centre on sulfoxide radical cation in the intermediate by electron releasing groups and facilitation of nucleophilic attack of water on the sulfoxide radical cation of PSAA by electron withdrawing groups. Additional evidence for the formation of sulfonium cation radical in the rate determining step *via* ET comes from the rate enhancement by the addition of acid. It has been established that the

sulfur radical cation is stabilized by $[H^+]$. From the formation of diphenyl disulfone as the final product (Eq.7), it has been proposedthat major portion of sulfoxide cation radical is consumed by the solvent water (Eq.4) followed by electron transfer and fragmentation. The sulfoxide radical formed as a result of nucleophilic attack of water on sulfoxide cation radical (Eq. 3)is followed by second electron transfer by another $[Fe(NN)_3]^{3+}$ (Eq. 5).

3.7 Interpretation of micellar effect

The decrease in reaction rate at higher surfactant concentrations is seen in most of the micelle catalyzed bimolecular reactions. This may be due to the dilution of the reactant molecules in the micellar medium. At higher [surfactant] thoughthe total number of micelles is increased, the stoichiometric concentrations of the substrate and the oxidant in and around Stern layer of micellar surface are decreased. As a result, the net concentration of the reactants is diluted with the increase in the concentration of surfactants and thereby causing a decrease in the reaction rate.

The observed increase in rate with increase in concentration of TX-100 at low concentrations clearly shows that the reaction takes place in micellar medium and both the reactants are associated or incorporated into micellar phase. In the present reaction PSAA is a neutral molecule and the other one is a cationic species. The neutral PSAA molecule can concentrate in the micellar phase by hydrophobic interaction or hydrogen bonding or both together. PSAA has carboxyl hydrogen which can form hydrogen bond with TX-100 through its oxyethylene oxygen atom. Because of this hydrogen bond, the stoichiometric concentration of thereactant molecule, PSAA increases at the Stern layer of TX-100.

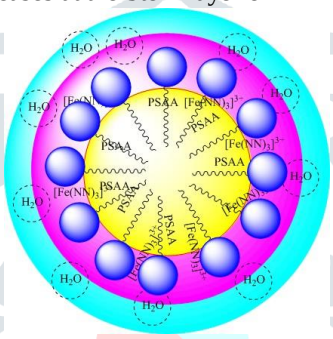

Figure 9. Schematic representation of reactants position in TX-100.

The oxidant, $[Fe(NN)_3]^{3+}$ cation also bind to the neutral head groups of TX-100 by a weak electrostatic attraction and thus the reactants PSAA and $[Fe(NN)_3]^{3+}$ are lying closer together in the stern layer of the micelle by hydrogen bonding and electrostatic force of attraction respectively. These are schematically represented in Figure 9. Because of their closer proximity in micellar medium, the reactants react fasterthan in aqueous media. At low concentrations of TX-100, the extent of positioning of the reactants and their stoichiometric concentration in micellar phase increase which result in an increase in rate constant.

3.8 Quantitative treatment using kinetic models

In the quantitative investigation of micellar catalysis and interactions, it is desirable to determine the binding constants for the formation of the substrate - micelle complex and the nature of the environment of the substrate in the molecular aggregate. Among the several quantitative models in the literature, the following models satisfactorily explain the micellar effect.

1. Menger Portnoy model
2. Piszkiewicz model
3. Raghvan and Srinivasan model and
4. Berezin model

In this section, the observed micellar effects are explained by considering the distribution pattern of reactants between the micellar and aqueous phases by the applicability of pseudo-phase kinetic models. The pseudo-phase description of micellar rate effects involves the implicit assumption that micelles provide a discrete reaction environment. On this basis, an attempt is made to compare the rate constants in TX-100 medium with those in aqueous medium. The various pseudo-phase models have been applied largely to quantitative aspects of reactivity in TX-100 medium between two distinct regions, *viz*., the aqueous and micellar pseudo-phases.

3.8.1. Menger-Portnoy model

Menger and Portnoy proposed the first kinetic model which treated micelles an enzyme like particles and applied successfully for both micellar and catalysts inhibited bimolecular reactions. The rate enhancement observed in many reactions upon addition of surfactants has been explained on the basis of the Scheme 2. The pseudo-phase model treats the overall reaction rate as the sum of rates in the aqueous and micellar pseudo-phases.

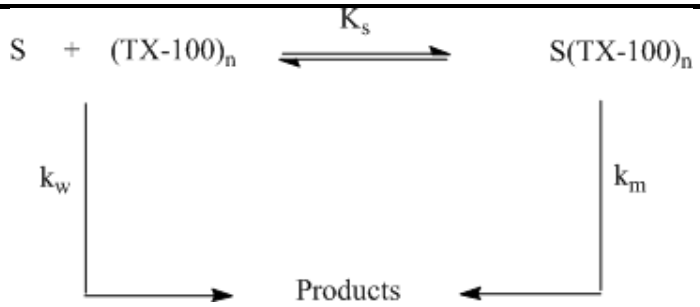

Scheme 2. Menger-Portnoy model.

In this scheme, K_s is the binding constant of the substrate to micellized surfactant, k_w and k_m are first order rate constants for ET reaction in the aqueous and micellar pseudo- phases. The Scheme 2 leads the rate law (8)

$$k_1 = \frac{k_w + k_m K_S [D_n]}{1 + K_S [D_n]} \quad (8)$$

The above equation on rearrangement gives Eq. 9

$$\frac{1}{k_1 - k_w} = \frac{1}{(k_m - k_w)} + \frac{1}{K_S (k_m - k_w) [D_n]} \quad (9)$$

$[D_n]$ is the total concentration of micellized surfactant, which is related to stoichiometric concentration of the surfactant $[D_T]$ and CMC as $[D_n] = [D_T] – CMC$. The CMC value of TX-100 (3×10^{-4} M), required for the calculation is taken from the literature (Hill 1910).

The validity of Menger-Portnoy model to TX-100 catalyzed reaction is obvious from the linear plots of $1/(k_1-k_w)$ *vs.*$1/[D_n]$ (Figure 10). The observed linearity with Menger-Portnoy model unambiguously proves that the PSAA partitions in both aqueous and TX-100 pseudo-phases. The reaction between PSAA and $[Fe(NN)_3]^{3+}$ is assumed to take place in both media according to Scheme 2.

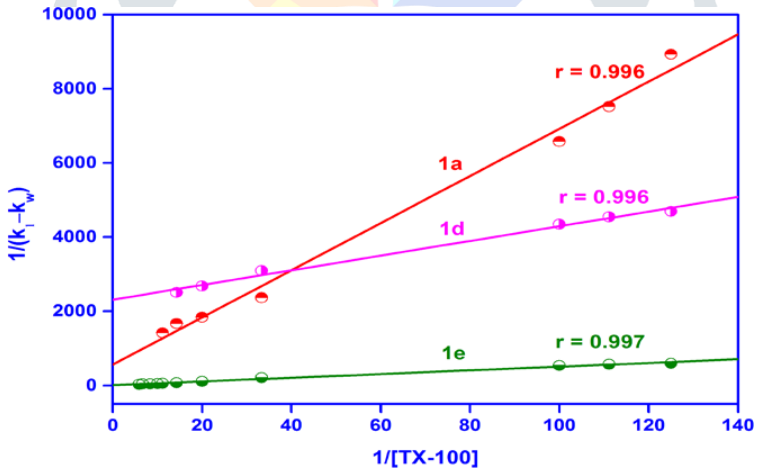

Figure 10. Linear Menger-Portnoy plots for different complexes

Table 4. Parameters evaluated from Menger-Portnoy plot

Complexes	K_s (M)	$10^4 k_m$ (s^{-1})
1a	8.9	10.5
1b	3.53	8.42
1c	18.7	15.9
1d	11.7	2.63
1e	1.803	110

The values of K_S and k_m evaluated from the slope and intercept of the linear plots are reported in Table 4. The mild rate

acceleration effect observed in TX-100 medium is evidenced by low binding constant values.

3.8.2 Piszkiewicz model

Reactions catalyzed by micelles have been viewed as models of enzyme-catalyzed reactions. This is based on the gross structural similarities and properties of micelles and enzymes and the fact that both micelles and enzymes bind the substrate witha non covalent interaction prior to the catalytic step (Raghavan & Srinivasan, 1987). A sigmoid shaped curve is obtained when the rate constants of micelle-catalyzed reactions are plotted against micelle concentration. This behaviour is analogous to positive cooperativity usually observed inenzymatic reactions. A kinetic model analogous to the Hill model (Martinek et al 1977) of enzymatic reactions, assumed that a rate plateau is achieved at high micellar concentrations. Most of the bimolecular reactions catalyzed by micelles have rate maxima. At very high micelle concentrations, the rate of the reactions decreases with increasing micelle concentration.

The simple mathematical model used to describe the sigmoid shaped dependence of rate constant on micelle concentration begins with the assumption that the substrate PSAA (S) and, n number of micelle molecules of TX-100 (D) aggregate to form catalytic micelle, D_nS, which may then react to yield the product (Scheme 3).

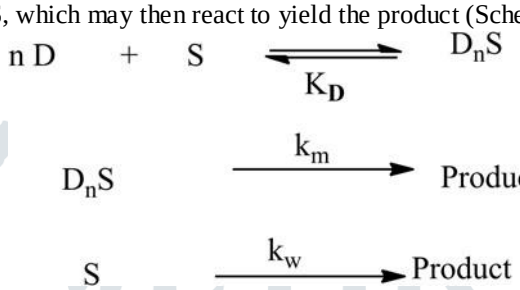

Scheme 3. Piszkiewicz kinetic model

K_D is the dissociation constant of the catalytic micelle back to its free components, k_m is the rate of electron transfer within TX-100 and k_w is the rate constant of reaction in the absence of TX-100.

$$k_1 = \frac{k_m[D]^n k_w K_D}{K_D + [D]^n} \quad (10)$$

The pseudo-first order rate constant as a function of micelle concentration is given by Eq. 10 which can be rearranged to Eq. 11

$$\log\left\{\frac{k_1 - k_w}{k_m - k_1}\right\} = n \log [D] - \log K_D \quad (11)$$

The term *n* is derived from experimental data as the slope of a plot of $\log [(k_1-k_w)/(k_m-k_1)]$ *vs.* $\log [D]$ (Berezin et al 1973), the intercept on the log [D] axis is $(\log K_D)/n$ and is equal to the concentration of TX-100 at which catalysis by TX-100 shows one-half its maximum effecton k_1.

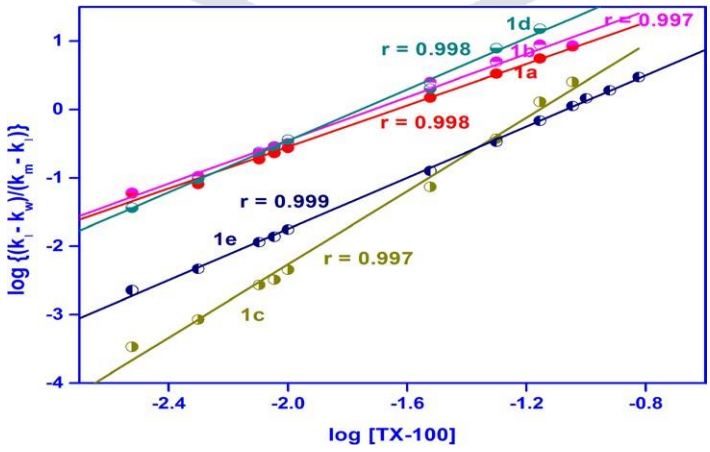

Figure 11. Piszkiewicz's plots for complexes **1a-1e** in TX-100.

Table 5. Piszkiewicz cooperativity values

Complex	Cooperativity Index (n)	$-\log[D]_{50}$	$10^2 [D]_{50}$	$10^3 K_D$	$10^{-2} 1/K_D$
1a	1.52	1.64	2.29	3.23	3.09

1b	1.58	1.71	1.92	1.95	5.11
1c	2.68	1.16	6.96	0.79	12.61
1d	1.87	1.76	1.72	0.500	19.99
1e	1.87	1.07	8.58	10.1	0.98

The rate constants of bimolecular reactions often decrease in the range of very high micellar concentration. This phenomenon may be analogous to substrate inhibition of an enzymatic reaction. At very high micelle concentrations, the substrate and micelle reverse their roles so that inhibition by micelle is seen. The overall reaction scheme which describes these bimolecular micelle-catalyzed reactions is given below in the Scheme 4.

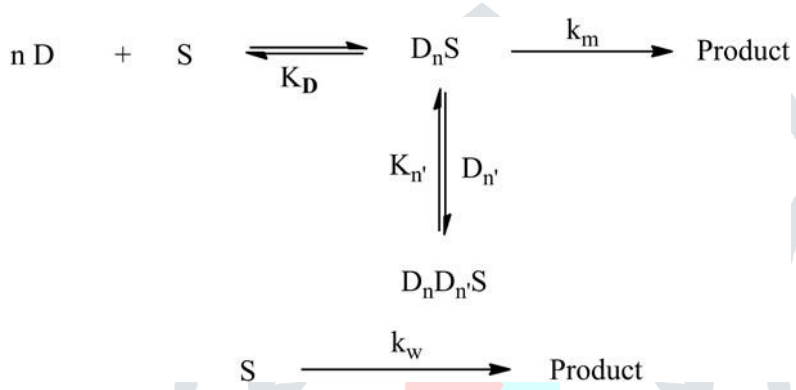

Scheme 4. Piszkiewicz model at high [micelle].

Here n' is the additional number of micellar molecules which associate with the catalytic micelle, D_nS to inactivate it, and K'_n is the association constant for this interaction. The second reactant would be at a steady state concentration and react with the catalytic micelle, D_nS in the step defined by the rate constant k_m. The rate constant, k_2, for a bimolecular reaction catalyzed by a micelle is given by

$$k_2 = \frac{k_m[D]^n + k_w K_D}{K_D + [D]^n + K_{n'}[D]^n [D]^{n'}} \quad (12)$$

$$k_2 = \frac{k_m}{1 + K_{n'}[D]^{n'}} \quad (13)$$

When the concentrations of TX-100 is low, Eq. 11 reduces to Eq. 12 and at high micelle concentrations, 11 reduces to 13.

3.8.3 Raghvan and Srinavasan model

For bimolecular micelle-catalyzed reactions, the model of Raghvan and Srinavasan (Raghavan & Srinivasan, 1987) can be used for evaluating the binding constants of the reactants. The distribution of both PSAA (S) and $[Fe(NN)_3]^{3+}$ (O) in aqueous and micellar pseudo-phases is considered in this model. This model assumes that the substrate PSAA associates with surfactant aggregates to form an aggregated complex D_nS to which the $[Fe(NN)_3]^{3+}$ binds to give a ternary complex D_nSO which may react according to the following Scheme 5.

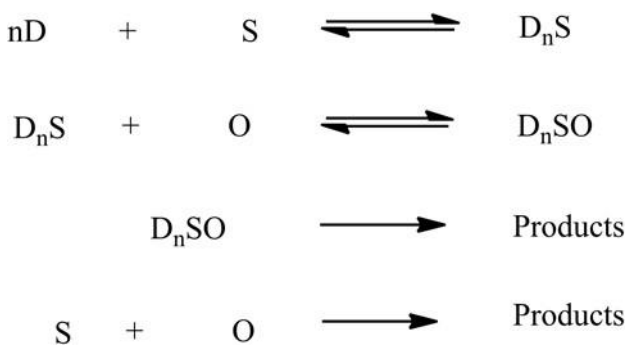

Scheme 5. Raghvan and Srinavasan kinetic model

According to this model, the observed rate constant in the presence of TX-100 is given bythe equation

$$k_1 = \frac{k_w + k_m K_S K_o [D]^n}{1 + K_S[D]^n\{1 + K_o[S]_T\}} \quad (14)$$

This equation is similar to those derived by Martinek et al (1977), Berezin et al (1973), and Bunton et al (1978). The Eq. 14 may be rearranged in the form (15).

$$\left[\frac{k_1 - k_w}{k_1}\right]\frac{1}{[D]^n} = K_s K_o\left[\frac{k_m}{k_1}\right] - K_s\{1 + K_o[S]_T\} \quad (15)$$

In Eq. 15, K_s and K_o are the binding constants of the substrate (PSAA) and the oxidant,$[Fe(NN)_3]^{3+}$, respectively. . The values of k_m and n are obtained from the linear plots of k_m/k_1 *vs.* $[(k_1-k_w)/k_1].1/[D]^n$ (Figure 12). Using the experimentally obtained k_w and the values of k_m and n from the Pizkiewicz model, the values of K_s and K_o are obtained using Eq. 15, and are tabulated in Table 6.

The evaluated values of K_S are in good agreement with $1/K_D$ obtained from Piszkiewicz model. The low values of K_o suggest that the $[Fe(NN)_3]^{3+}$ is present almost exclusively in the bulk aqueous phase. This idea is consistent with the assumptions of Raghavan (1987) and Reeves (1975). In view of the above observed results, the reaction is assumed to take place between the PSAA solubilized in micelle and the $[Fe(NN)_3]^{3+}$ residing at the Stern layer. The concentration of TX-100 significantly influences the extent of incorporation of the PSAA within the micelle.

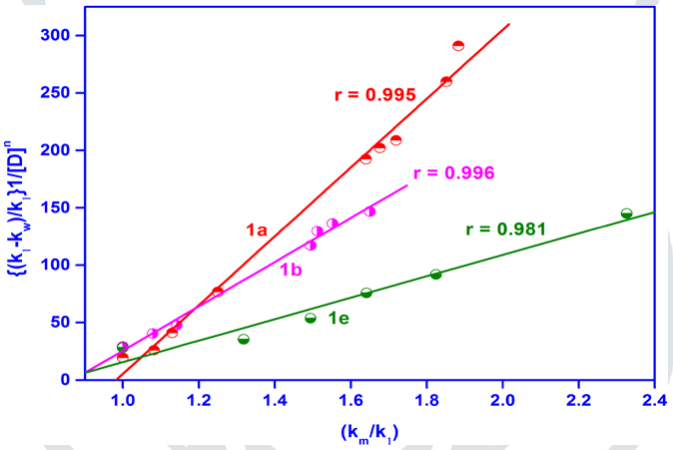

Figure 12. Raghvan and Srinivasan plots for different complexes in TX-100.

Table 6. Evaluated binding constants using Raghvan and Srinivasan model.

Complex	Cooperativity Index (n)	10^{-2} Intercept	10^{-2} K_s	K_o	10^{-2} $1/K_D$
1a	1.52	-2.94	2.94	1.02	3.09
1b	1.58	-1.67	1.67	1.15	5.11
1c	2.68	-5.75	5.75	1.33	12.61
1d	1.87	-18.8	18.8	1.01	19.99
1e	1.87	-1.64	1.64	0.76	0.98

3.8.4 Berezin model

Micellar catalysis by TX-100 critically depends on the interactions of TX-100 with PSAA and $[Fe(NN)_3]^{3+}$. Number of different interactions are involved includingthose associated with the head group of the TX-100, different segments of the polyethyleneoxy chain, and the counterions. In Berezin model (1973) a solution above the CMC is considered as two-phase system, consisting of an aqueous phase and a micellar pseudo-phase. According to this model, the reactants are assumed to distribute between bulk solvent and the micellar assemblies. The reaction is assumed to take place in two areas which are

considered as a separate reaction regions ie., as pseudo-phases. This canbe discussed in Scheme 6.

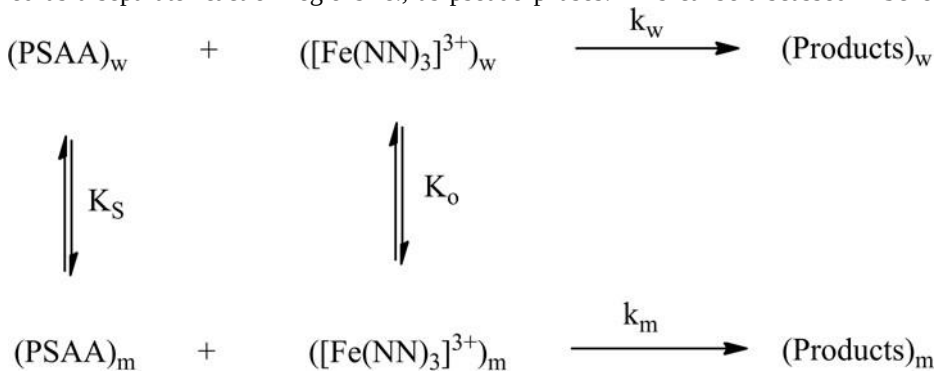

Scheme 6. Berezin model.

A quantitative rate expression for a bimolecular reaction occurring in aqueous and micellar phases according to this model is given as,

$$k_1 = \frac{k_w + k_m K_s K_o ([D]\text{-}CMC)}{[1+ K_s ([D]\text{-}CMC)][1+ K_o ([D]\text{-}CMC]} \quad (16)$$

where, K_s and K_o are the association constants of PSAA and $[Fe(NN)_3]^{3+}$ respectively with TX-100, [D] is the analytical concentration of TX-100 = (k_m/V), V being molar volume of the micelle and k_w and k_m are the pseudo-first-order rate constants in the absence and presence of TX-100, respectively. Since formation of hydrogen bonding is possible between the carboxylic hydrogen of PSAA and the oxyethylene oxygen of TX- 100, it may be expected that K_S will be high. K_O will also be high because of high hydrophobic interaction with $[Fe(NN)_3]^{3+}$. As the values of K_S and Ko are large and [D] is small, it may be possible that $k_w >> k_m K_s K_o$ ([D]-CMC) and the Eq. 17 takes the form.

$$k_1 = \frac{k_w}{[1+ (K_s+ K_o) [D]\text{-}CMC)] + K_s K_o ([D]\text{-}CMC)^2} \quad (17)$$

Again, since ([D]-CMC) is very small, the terms containing $([D]\text{-}CMC)^2$ may be neglected, and the Eq. (17) may be rearranged to

$$\frac{1}{k_1} = \frac{1}{k_w} + \frac{K_s + K_o}{k_w} ([D]\text{-}CMC) \quad (18)$$

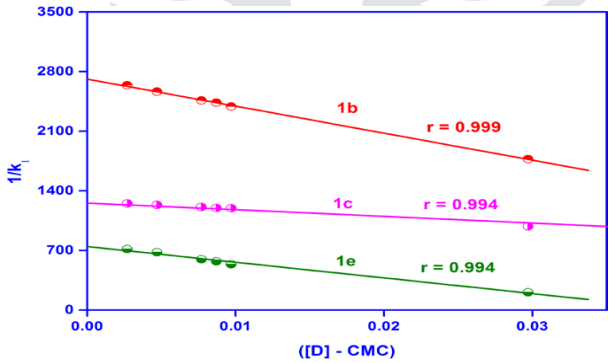

Figure 13. Applicability of Berezin model.

In the present study, the plot of k_1 *vs.* ([D]-CMC) (Figure 13) gave an excellent straight line which indicates the validity of Berezin model, confirming the occurrence of the reaction both in micellar and aqueous pseudo-phases. The negative slope indicates that the reaction is accelerated by TX-100. The values of Berezin parameters calculated from the linear plots are given in Table 7.

Table 7. Calculated parameters of Berezin model.

Complex	$10^4 k_w$ (s^{-1})	$K_s + K_o$
1a	7.10	18.31
1b	3.69	11.71
1c	7.96	6.249

1d	1.62	30.34
1e	13.42	24.69

4. CONCLUSION

The kinetics of the electron transfer reactions between PSAA and $[Fe(NN)_3]^{3+}$ were studied in the presence of nonionic surfactant, (TX-100) . The calculated low values of Michaelis-Menten constant (K_m) ensures that strong binding of PSAA to the iron(III) polypyridyl complexes during intermediate formation in TX-100 medium. On applying the Hammett substituent constants to the overall rate constants obtained in TX-100 medium, non-linear concave upward Hammett plots were obtained. The rate enhancement observed in the electron transfer reaction between PSAA and $[Fe(NN)3]^{3+}$ in TX-100 is attributed to the hydrogen bonding and hydrophobic interaction occurring between the surfactant and reactants. A suitable mechanism with the formation of Diphenyl sulfone as the product has been proposed. Application of different kinetic models confirms the behavior of micellar catalyzed reactions.

ACKNOWLEDGEMENT

RJER thanks the UGC, SERO, Hyderabad, the Management of Nazareth Margoschis College and Manonmaniam Sundaranar University for the award of a fellowship under FDP. The authors gratefully thank the Management, Aditanar College of Arts and Science, Tiruchendur for providing Laboratory facilities to do the research.

5.REFERENCES

[1]	Adaikalasamy, K.J. Venkataramanan N.S. and Rajagopal, S. (2003) Electron transfer reactions of iron(III)-polypyridyl complexes with organic sulfoxides, Tetrahedron, 59(20), 3613-3619.
[2]	Alhaji, N.M.I., Mohideen, A.M.U. and Kalaimathi, K. (2011) Mechanism of Oxidation of (p-Substituted Phenylthio)acetic Acids with N-Bromophthalimide, E-Journal of Chemistry, 8(1), 1-8.
[3]	Altaf, M. and Jaganyi, D. (2013) Oxidation of Methionine by Colloidal MnO_2 in Aqueous and Micellar Media: A Kinetic Study, Journal of Dispersion Science and Technology, 34(11), 1481-1487.
[4]	Anitha, N. and Palaniandavar, M. (2011) Mononuclear iron(III) complexes of 3N ligands in organized assemblies: spectral and redox properties and attainment of regioselective extradiol dioxygenase activity, Dalton Transactions, 40 (9), 1888-1901.
[5]	Balakumar, P., Balakumar, S. and Subramaniam, P. (2012) Der. Chemica Sinica 4, 959-964.
[6]	Balakumar, S., Thanasekaran, P., Rajagopal, S. and Ramaraj, R. (1995) Tetrahedron, Electron transfer reactions of iron (III) - polypyridyl complexes with organic sulphides, 51(16), 4801–4818.
[7]	Berezin, I.V., Martinek, K. and A.K. Yatsimirski, (1973) Physicochemical foundations of micellar catalysis, Russian Chemical Reveiws, 42(10), 787.
[8]	Bunton, C.A.., Rivera, F. and Sepulveda, l. (1978) Micellar effects upon the hydrogen ion and general acid catalyzed hydration of 1,4-dihydropyridines,The Journal of Organic Chemistry, 43(6), 1166-1173.
[9]	Deepalakshmi, S., Sivalingam, A,. Kannadasan, T,. Subramaniam, P., Sivakumar P. and T. Brahadeesh, S. (2014) Spectroscopic investigation on kinetics, thermodynamics and mechanism for electron transfer reaction of iron(III) complex with sulphur centered radical in stimulated biological system, Spectrochimica Acta, A: Molecular and Biomolecular Spectroscopy, 124, 315-321.
[10]	Frescura, V., Marconi, D.M.O., Zanette, D., Nome, F., Blasco, A. and Bunton, C.A. (1995) Effects of Sulfobetaine-Sodium Dodecanoate Micelles on Deacylation and Indicator Equilibrium, Journal of Physical Chemistry, 99(29), 11494-11500.
[11]	Gangwar, S.K. and Rafiquee, M.Z.A. (2007) Kinetics of the alkaline hydrolysis of fenuron in aqueous and micellar media, International Journal of Chemical Kinetics, 39(11), 638 -644.
[12]	Hey, M.H. (1982) Mineralogical Magazine, 46(341), 512.
[13]	Hill, A.V. (1910) A new mathematical treatment of changes of ionic concentration in muscle and nerve under the action of electric currents, with a theory as to their mode of excitation, The Journal of Physiology, 40(3), 190- 224.
[14]	Jeevi Esther Rathnakumari, R., Kavitha, C., Vetriselvi, V., Subramaniam, P. and Janet Sylvia Jaba Rose, J. (2024) Non-linear Hammett in the SDS mediated electron transfer reactions in the oxidation of Phenylsulfinylacetic acid by Iron(III) polypyridyl complexes, International Journal of Creative Research Thoughts, 12, c633-c645
[15]	Martinek, K., Yatsimirski, A.K., Lavashor, A.V. and Berezin I.V. (1977) Micellization, Solubilization and Microemulsion, Vol. 2, K.L. Mittal, (ed.), Plenum Press, New York, 489.
[16]	Nagaonkar, U.C. and Bhagwat, S.S. (2007) Selective Reduction of Isophorone in Micellar Media, Industrial and Engineering Chemistry Research, 46(7), 1923-1927.

[17]	Pal, S.K. Peon, J. Bagchi, B. and Zewail, A.H. (2002) Biological Water: Femtosecond Dynamics of Macromolecular Hydration, The Journal of Physical Chemistry: B, 106(48), 12376-12395.
[18]	Pawar, B. and Bhagwat, S. (2012) Micelle Catalyzed Monosulfonylation of Amines and Amino Acids in Aqueous Media, Journal Surface Science and Technology, 28(3-4), 111-131.
[19]	Raghavan, P.S. and Srinivasan, V.S. (1987) Kinetic model for micellar catalysed hydrolysis of esters-biomolecular reactions, Journal of Chemical Sciences, 98, 199-206.
[20]	Reeves, R.L. (1975) Nature of mixed micelles from anionic dyes and cationic surfactants. Kinetic study, Journal of the American Chemical Society, 97(21), 6019-6024.
[21]	Rumki, N., Aniruddha, G., Susanta, M. and Saha, B. (2015) Micellar Catalysis on 1,10-Phenanthroline Promoted Chromic Acid Oxidation of Dimethyl Sulfoxide to Dimethyl Sulfone in Aqueous Media at Room Temperature, Journal of Thermodynamics and Catalysis, 6(2), 1000145.
[22]	Saha, R. Ghosh, A. and Saha, B. (2013) Kinetics of micellar catalysis on oxidation of *p*-anisaldehyde to *p*-anisic acid in aqueous medium at room temperature, Chemical Engineering Science, 99, 23-27.
[23]	Schmid, R. and Han, L. (1983) Novel mechanistic aspects of the reduction of iron(III) phenanthroline complexes by aquo iron(II). Temperature dependence of the substituent effect, Inorganica Chimica Acta, 69, 127-134
[24]	Shrikhande, J.J., Gawande, M.B. and Jayaram, R.V. (2008) A catalyst-free N-benzyloxycarbonylation of amines in aqueous micellar media at room temperature, Tetrahedron Letters, 49(32), 4799-4803.
[25]	Singh, M. (2012) Oxidative Degradation of D-Sucrose by Employing N-Bromosuccinimide as Oxidant: A Micellar Kinetic and Catalytic Study, Synthesis and Reactictivity in Inorganic, Metal- Organic and Nano-Metal Chemistry, 42(9), 1315-1326.
[26]	Subramaniam, P. and Thamil Selvi, N. (2014) Micellar and Substituent Effects on the Redox Reactions of Phenylsulfinylacetic Acid and Cr (VI) in SDS Medium, International Journal of Advanced Scientific Research, 4, 418-421.
[27]	Subramaniam, P. and Thamil Selvi, N. (2015) Dynamics of cetyltrimethylammonium bromide-mediated reaction of phenylsulfinylacetic acid with Cr(VI): Treatment of pseudo-phase models, Journal of the Serbian Chemical Society, 80(8); 1019-1034.
[28]	Subramaniam, P., Janet Sylvia Jabarose, J. and Jeevi Esther Rathnakumari R. (2016) A paradigm shift in rate determining step from single electron transfer between phenylsulfinylacetic acids and iron(III) polypyridyl complexes to nucleophilic attack of water to the produced sulfoxide radical cation: a non-linear Hammett, Journal of Physical Organic Chemistry, 29(10): 496-504.
[29]	Thenraja, D., Subramaniam, P. and Srinivasan, C. (2002) Kinetics and mechanism of oxygenation of aromatic sulfides and arylmercaptoacetic acids by peroxomonophosphoric acid, Tetrahedron 58(21), 4283-4290.